Structural Engineering and Mechanics, Vol. 40, No. 3 (2011) 347-371
DOI: http://dx.doi.org/10.12989/sem.2011.40.3.347

Post-buckling analysis of Timoshenko beams with various boundary conditions under non-uniform thermal loading

Turgut Kocatürk* and Şeref Doğuşcan Akbaş[a]

Department of Civil Engineering, Yildiz Technical University, Davutpasa Campus, 34210 Esenler-İstanbul, Turkey

(Received December 1, 2010, Revised April 5, 2011, Accepted August 17, 2011)

Abstract. This paper focuses on post-buckling analysis of Timoshenko beams with various boundary conditions subjected to a non-uniform thermal loading by using the total Lagrangian Timoshenko beam element approximation. Six types of support conditions for the beams are considered. The considered highly non-linear problem is solved by using incremental displacement-based finite element method in conjunction with Newton-Raphson iteration method. As far as the authors know, there is no study on the post-buckling analysis of Timoshenko beams under uniform and non-uniform thermal loading considering full geometric non-linearity investigated by using finite element method. The convergence studies are made and the obtained results are compared with the published results. In the study, the relationships between deflections, end rotational angles, end constraint forces, thermal buckling configuration, stress distributions through the thickness of the beams and temperature rising are illustrated in detail in post-buckling case.

Keywords: geometrical non-linearity; post-buckling analysis; total lagrangian finite element model; Timoshenko beam; non-uniform temperature rise

1. Introduction

Aerospace vehicles, nuclear power plants, thermal power plants etc. are subject to thermal loadings. In the case of beams with immovable ends, temperature rise causes compressible forces end therefore buckling phenomena occurs. In recent years, much more attention has been given to the thermal buckling of beam structures. Rao and Raju (1984) investigated thermal postbuckling of columns.

Global descriptions of the properties of buckled states of nonlinearly thermoelastic beams and plates when heated at their ends and edges is investigated by Gauss and Antman (1984). Jekot (1996) investigated the thermal postbuckling of a beam made of physically nonlinear thermoelastic material by using the geometric equations in the von-Karman strain-displacement approximation. Li (2000) examined Thermal Post-Buckling of Rods with Pinned-Fixed Ends using the shooting method. Coffin and Bloom (1999) gave an elliptic integral solution for the symmetric post-buckling response of a linear elastic and hygrothermal beam with the two ends pinned. On the basis of exact

Corresponding author, Professor, E-mail: kocaturk@yildiz.edu.tr
[a]Research Assistant

nonlinear geometric theory of extensible beam and by using a shooting method, computational analysis for thermal post buckling behavior of beams with pinned-pinned, fixed-fixed and pinned-fixed ends were presented by Li and Cheng (2000), Li *et al*. (2002) and Li and Zhou (2001). Thermal post-buckling responses of an elastic beam, with immovably simply supported ends and subjected to a transversely non-uniformly distributed temperature rising, were investigated by Li *et al.* (2003). Thermal post-buckling response of an immovably pinned-fixed Timoshenko beam subjected to a static transversely nonuniform temperature rise is numerically analyzed by using a shooting method by Li and Zhou (2003).

Based on the finite element method, the analysis of heat conduction and structural stress and buckling are considered at the same time in the design optimization procedure by Chen *et al*. (2003). Vaz and Solano (2003, 2004) investigated thermal post-buckling of rods and came up with a closed form solution via uncoupled elliptical integrals. Large thermal deflections for Timoshenko beams subjected to transversely non-uniform temperature rise and with pinned-pinned as well as fixed-fixed ends are numerically analyzed by Li and Song (2006). Aristizabal-Ochao (2007) developed a new set of slope deflection equations for Timoshenko beam-columns which includes the combined effects of shear and bending deformations, and second-order axial load effects in a classical manner and emphasized the great importance of shear effects on static, tension and compression stability and dynamic behavior of elastomeric bearings used for seismic isolation. Both thermal buckling and post-buckling of pinned-fixed beams resting on an elastic foundation are investigated by Song and Li (2007). Vaz *et al.* (2007) examined a perturbation solution for the initial post-buckling of beams that were supported on an elastic foundation under uniform thermal load. The large-deflection analysis and post-buckling behavior of laterally braced or unbraced slender beam-columns of symmetrical cross section subjected to end loads (forces and moments) with both ends partially restrained against rotation, including the effects of out-of-plumbness and a new set of slope-deflection equations for Timoshenko beam-columns of symmetrical cross section with semi-rigid connections that include the combined effects of shear and bending deformations, and second-order axial load effects are developed in a classical manner by Aristizabal-Ochao (2008). Evandro and Joao (2008) investigated a simple and efficient methodology for sensitivity analysis of geometrically nonlinear structures subjected to thermo-mechanical loading in regular and critical states. Thermal post-buckling analysis of uniform, isotropic, slender and shear flexible columns is presented using a rigorous finite element formulation and a much simpler intuitive formulation by Gupta *et al*. (2009). Gupta *et al*. (2010) investigated simple, elegant, and accurate closed-form expressions for predicting the post-buckling behavior of composite beams with axially immovable ends using the Rayleigh-Ritz method. Thermal post-buckling analysis of columns with axially immovable ends is studied using the Rayleigh-Ritz method by Gupta *et al*. (2010). Vaz *et al*. (2010) examined a perturbation solution for the initial post-buckling behavior of slender beams that were assumed to be double-hinged with fixed ends, preventing thermal expansion. Akbaş and Kocatürk (2011) investigated post-buckling analysis of a simply supported beam subjected to a uniform thermal loading by using total Lagrangian finite element model of two dimensional continuum for an eight-node quadratic element.

As far as the authors know, there is no study on the post-buckling analysis of Timoshenko beams under uniform and non-uniform thermal loading considering full geometric non-linearity investigated by using finite element method: Gupta *et al*. (2009) investigated the post-buckling analysis of beams under thermal loading by using finite element method and von-Karman strain-displacement approximation in which full geometric non-linearity cannot be considered. In von

Karman nonlinear strain approximation, because of neglect of some components of strain, satisfactory results can be obtained only for large displacements but moderate rotations. In the present study, the post buckling analysis of Timoshenko beams under non-uniform thermal loading with various boundary conditions is considered by using total Lagrangian finite element method in which full geometric nonlinearity can be considered as distinct from the study of Gupta *et al*. (2009).

The development of the formulations of general solution procedure of nonlinear problems follows the general outline of the derivation given by Zienkiewichz and Taylor (2000). The related formulations of post-buckling analysis of Timoshenko beams with various boundary conditions subjected to a non-uniform thermal loading are obtained by using the total Lagrangian finite element model of Timoshenko beam. Convergence studies are performed for various numbers of elements. In deriving the formulations for post buckling analysis under non-uniform thermal loading, the total Lagrangian Timoshenko beam element formulations given by Felippa (2010) are used. There is no retstriction on the magnitudes of deflections and rotations in contradistinction to von-Karman strain displacement relations of the beam. The relationships between deflections, end rotational angles, end constraint forces, thermal buckling configuration, stress distributions through the thickness of the beams and temperature rising are illustrated in detail in post-buckling case. Convergence study is performed for various numbers of elements.

2. Theory and formulations

The various beam configurations, made of isotropic, elastic material, with co-ordinate system $O(XYZ)$, considered in the present study are shown in Fig. 1 and their boundary conditions are given in Table 1.

While the derivation of the governing equations for most problems is not unduly difficult, their solution by exact methods of analysis is a formidable task. In such cases, numerical methods of analysis provide an alternative means of finding solutions. Numerical methods typically transform differential equations to algebraic equations that are to be solved by using computers. The considered problem is a nonlinear one. Even linear problems may not admit exact solutions due to geometric and material complexities, but it is relatively easy to obtain approximate solutions using numerical methods (Reddy 2004). There are some solutions for the special cases of boundary and loading conditions for large displacements of beams in the framework of Euler-Bernoulli beam theory. For the solution of the total Lagrangian formulations of TL plane beam problem, small-step incremental approaches from known solutions are used. In this study, the TL Timoshenko beam element is used and the related formulations are developed by using the formulations given by Felippa (2010). In the present study, finite element model of Timoshenko beam element is developed by using a two-node beam element shown in Fig. 2. Each node has three degrees of freedom: Two node displacements u_{xi} and u_{yi}, and one rotation θ_i about Z axis.

A particle originally located at $P_0(X, Y)$ moves to $P(x, y)$ in the current configuration, as shown in Fig. 3. The projections of P_0 and P along the cross sections at C_0 and C upon the neutral axis are called $C_0(X, 0)$ and $C(x_c, y_c)$, respectively. It will be assumed that the cross section of the beam dimensions do not change, and that the shear distortion $\gamma << 1$ so that $\cos\gamma$ can be replaced by 1. Then Felippa (2010)

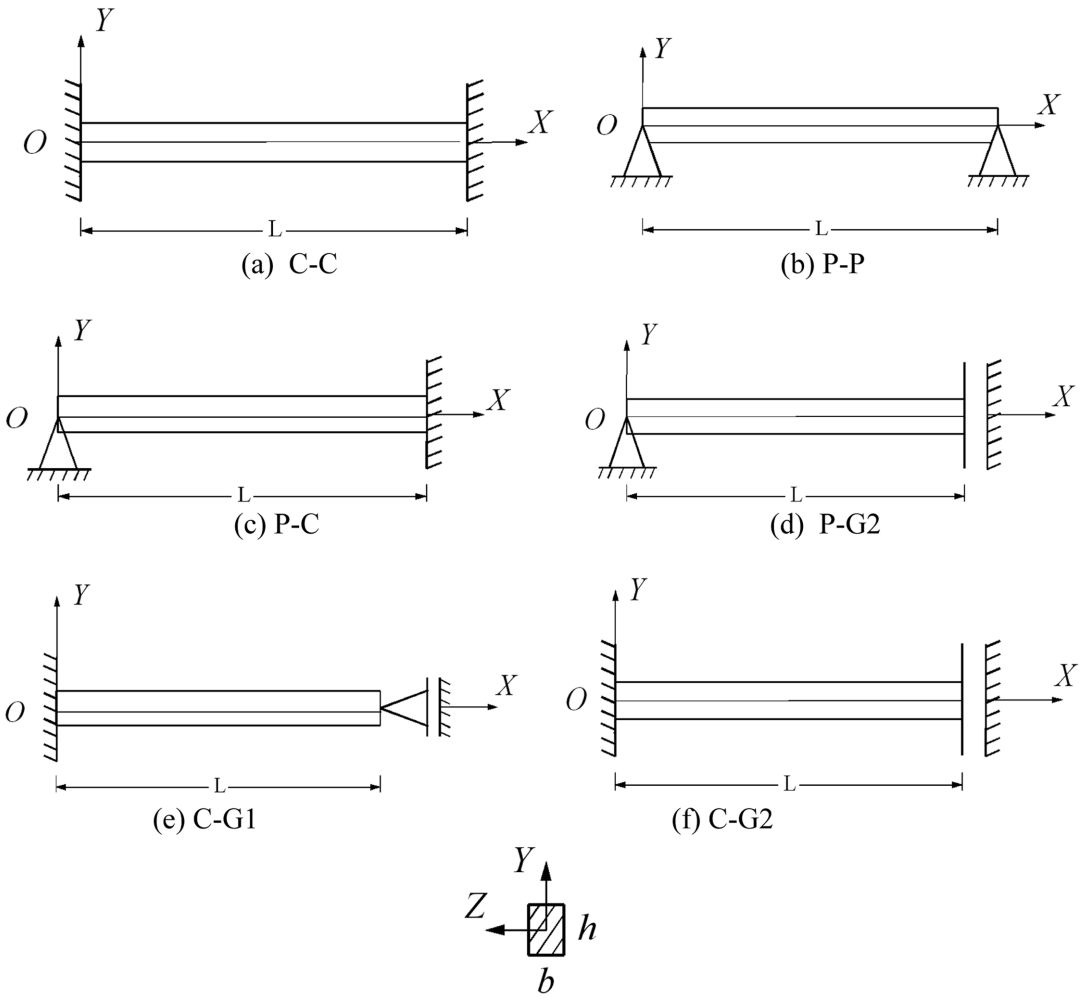

Fig. 1 Beams with various boundary conditions

Table 1 Boundary conditions of the beams

Boundary configurations	Boundary conditions
P-P	$u_X(0) = u_X(L) = u_Y(0) = u_Y(L) = 0$
C-C	$u_X(0) = u_X(L) = u_Y(0) = u_Y(L) = \theta(0) = \theta(L) = 0$
P-C	$u_X(0) = u_X(L) = u_Y(0) = u_Y(L) = \theta(L) = 0$
P-G2	$u_X(0) = u_X(L) = u_Y(0) = \theta(L) = 0$
C-G1	$u_X(0) = u_X(L) = u_Y(0) = \theta(0) = 0$
C-G2	$u_X(0) = u_X(L) = u_Y(0) = \theta(0) = \theta(L) = 0$

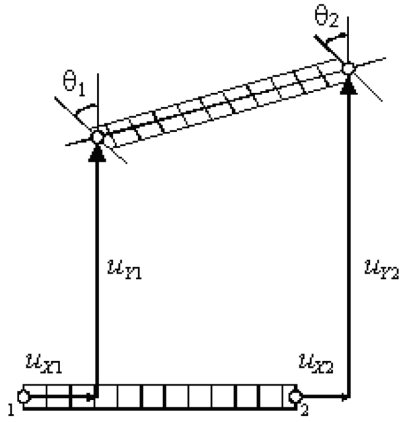

Fig. 2 A two-node C^0 beam element

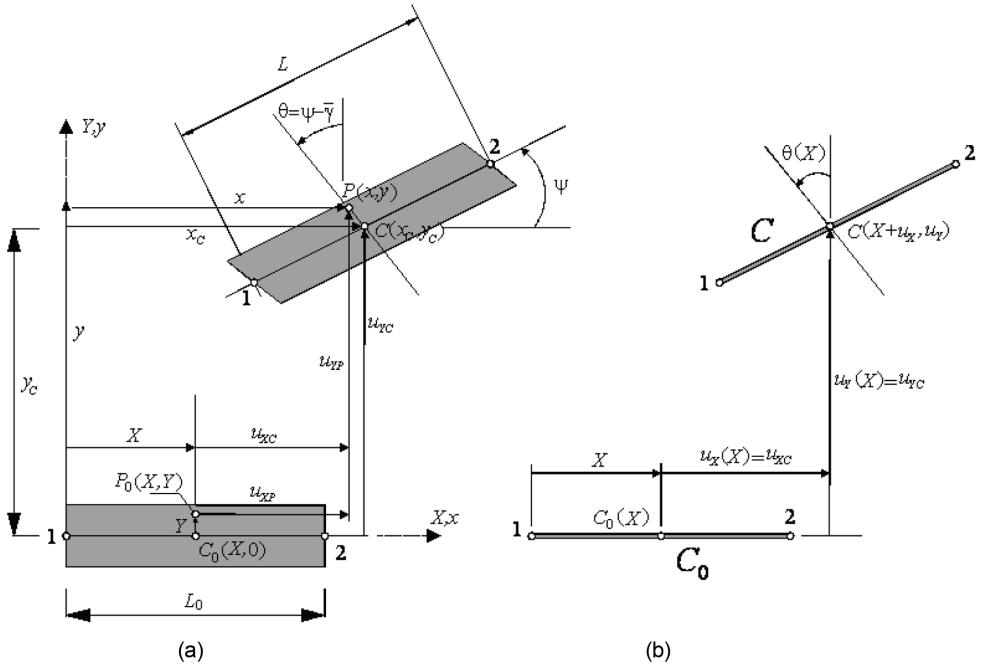

Fig. 3 Lagrangian kinematics of the C^0 beam element with X-aligned reference configuration: (a) plane beam moving as a two-dimensional body, (b) reduction of motion description to one dimension measured by coordinate X. This Fig. is given by Felippa (2010)

$$x = x_c - Y(\sin\psi + \sin\gamma\cos\psi) = x_c - Y[\sin(\psi+\gamma) + (1-\cos\gamma)\sin\psi] = x_c - Y\sin\theta \tag{1}$$

$$y = y_c + Y(\cos\psi - \sin\gamma\sin\psi) = y_c + Y[\cos(\psi+\gamma) + (1-\cos\gamma)\cos\psi] = y_c + Y\cos\theta \tag{2}$$

where $x_c = X + u_{XC}$ and $y_c = u_{XC}$. Consequently, $x = X + u_{XC} - Y\sin\theta$ and $y = u_{YC} + Y\cos\theta$. From now on we shall call u_{XC} and u_{YC} simply u_X and u_Y, respectively, so that the Lagrangian representation of the motion is

$$\begin{bmatrix} x \\ y \end{bmatrix} = \begin{bmatrix} X + u_x - Y\sin\theta \\ u_y + Y\cos\theta \end{bmatrix} \tag{3}$$

in which u_X, u_Y and θ are functions of X only. This concludes the reduction to a one-dimensional model, as sketched in Fig. 3(b). For a two-node C_0 element, it is natural to express the displacements and rotation functions as linear in the node displacements

$$\mathbf{w} = \begin{bmatrix} u_X(X) \\ u_Y(X) \\ \theta(X) \end{bmatrix} = \frac{1}{2}\begin{bmatrix} 1-\xi & 0 & 0 & 1+\xi & 0 & 0 \\ 0 & 1-\xi & 0 & 0 & 1+\xi & 0 \\ 0 & 0 & 1-\xi & 0 & 0 & 1+\xi \end{bmatrix}\begin{bmatrix} u_{X1} \\ u_{Y1} \\ \theta_1 \\ u_{X2} \\ u_{Y2} \\ \theta_2 \end{bmatrix} = \mathbf{N}\mathbf{u} \tag{4}$$

in which $\xi = (2X/L_0) - 1$ is the isoparametric coordinate that varies from $\xi = -1$ at node 1 to $\xi = 1$ at node 2.

The Green-Lagrange strain-displacement relations are given by Felippa (2010) as follows

$$\mathbf{e} = \begin{bmatrix} e_1 \\ e_2 \end{bmatrix} = \begin{bmatrix} e_{XX} \\ 2e_{XY} \end{bmatrix} = \begin{bmatrix} (1+u'_X)\cos\theta + u'_Y\sin\theta - Y\theta' - 1 \\ -(1+u'_X)\sin\theta + u'_Y\sin\theta \end{bmatrix} = \begin{bmatrix} e - Y\kappa \\ \gamma \end{bmatrix} \tag{5}$$

$$\kappa = \theta' = \frac{\theta_2 - \theta_1}{L_0};\ e = (1+u'_X)\cos\theta + u'_Y\sin\theta - 1;\ \gamma = -(1+u'_X)\sin\theta + u'_Y\cos\theta \tag{6}$$

where e is the axial strain, γ is the shear strain, κ is curvature of the beam, $u'_X = du_X/dX$, $u'_Y = du_Y/dX$, $\theta' = d\theta/dX$. The second Piola-Kirchhoff stresses with a non-uniform temperature rise can be expressed as follows

$$\mathbf{s} = \begin{bmatrix} s_{XX} \\ s_{XY} \end{bmatrix} = \begin{bmatrix} s_1 \\ s_2 \end{bmatrix} = \begin{bmatrix} s_1^0 + E(e_1 - \alpha_X T) \\ s_2^0 + Ge_2 \end{bmatrix} = \begin{bmatrix} s_1^0 \\ s_2^0 \end{bmatrix} + \begin{bmatrix} E & 0 \\ 0 & G \end{bmatrix}\begin{bmatrix} e_1 - \alpha_X T \\ e_2 \end{bmatrix} \tag{7}$$

where s_1^0, s_2^0 are initial stresses, E is the modulus of elasticity, G is the shear modulus, α_X is coefficient of thermal expansion in the X direction, T is the temperature. Variation of the temperature along the beam height can be expressed as

$$T = \frac{T_T + T_B}{2} + \frac{(T_T - T_B)}{h}Y = T_M + \frac{T_D}{h}Y \quad -0.5h \le Y \le 0.5h \tag{8}$$

where T_T and T_B are the temperature rise of the top and the bottom surfaces of the beam, $T_M = T_T + T_B/2$ is the average value of the top and bottom temperature rising, $T_D = (T_T - T_B)$ is the difference value of the top and bottom temperature rise. In this study, $T_D \ge 0$.

Using constitutive equations, axial force N, shear force V and bending moment M can be obtained as

$$N = \int_A s_1 dA = \int_A [s_1^0 + E(e_1 - \alpha_X T)]dA = N^0 + EeA - E\alpha_X\left(\frac{T_T + T_B}{2}\right)A \tag{9}$$

$$V = \int_A s_2 dA = \int_A [s_2^0 + Ge_2] dA = V^0 + A_0\gamma \tag{10}$$

$$M = \int_A -Ys_1 dA = \int_A -Y[s_1^0 + E(e_1 - \alpha_X T)] dA = M^0 + EI_0\left(\kappa + \alpha_X \frac{(T_T - T_B)}{h}\right) \tag{11}$$

where

$$N^0 = \int_{A_0} s_1^0 dA\,, \quad V^0 = \int_{A_0} s_2^0 dA\,, \quad M^0 = \int_{A_0} -Ys_1^0 dA \tag{12}$$

The element tangent stiffness matrix for the total Lagrangian Timoshenko plane beam element is as follows which is given by Felippa (2010)

$$\mathbf{K}_T = \mathbf{K}_M + \mathbf{K}_G \tag{13}$$

where $\mathbf{K}_G$ is the geometric stiffness matrix, and $\mathbf{K}_M$ is the material stiffness matrix given as follows by Felippa (2010)

$$\mathbf{K}_M = \int_{L_0} \mathbf{B}_m^T \mathbf{S} \mathbf{B}_m dX \tag{14}$$

After integration of Eq. (14), $\mathbf{K}_M$ can be expressed as follows

$$\mathbf{K}_M = \mathbf{K}_M^a + \mathbf{K}_M^b + \mathbf{K}_M^s \tag{15}$$

where $\mathbf{K}_M^a$ is the axial stiffness matrix, $\mathbf{K}_M^b$ is the bending stiffness matrix, $\mathbf{K}_M^s$ is the shearing stiffness matrix and $\mathbf{B}_m$ is

$$\mathbf{B}_m = \mathbf{B}|_{\xi=0} = \frac{1}{L_0}\begin{bmatrix} -c_m & -s_m & -\frac{1}{2}L_0\gamma_m & c_m & s_m & -\frac{1}{2}L_0\gamma_m \\ s_m & -c_m & \frac{1}{2}L_0(1+e_m) & s_m & -c_m & \frac{1}{2}L_0(1+e_m) \\ 0 & 0 & -1 & 0 & 0 & 1 \end{bmatrix} \tag{16}$$

where m stands for beam midpoint, $\xi = 0$, and $\theta_m = (\theta_1 + \theta_2)/2$, $\omega_m = \theta_m + \varphi$, $c_m = \cos\omega_m$, $s_m = \sin\omega_m$, $e_m = L\cos(\theta_m - \psi)/L_0 - 1$, and $\gamma_m = L\sin(\psi - \theta_m)/L_0$ (See Fig. 4 for symbols). The axis of the considered beam initially is taken as horizontal, therefore $\varphi = 0$. The matrix $\mathbf{S}$ is defined as follows

$$\mathbf{S} = \begin{bmatrix} EA_0 & 0 & 0 \\ 0 & GA_0 & 0 \\ 0 & 0 & EI_0 \end{bmatrix} \tag{17}$$

Performing the integral in Eq. (14) gives

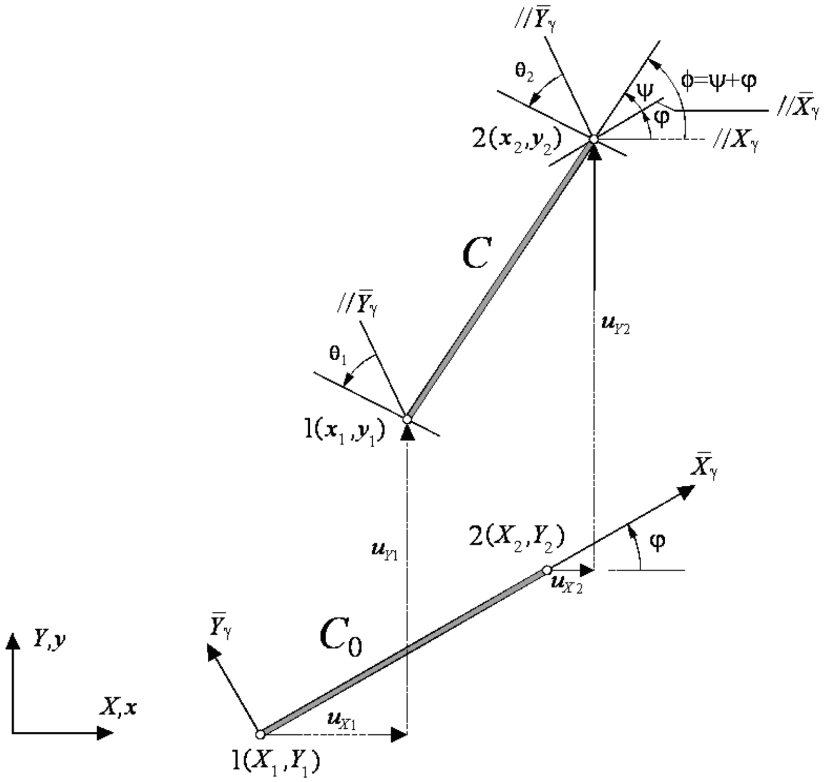

Fig. 4 Plane beam element with arbitrarily oriented reference configuration. This figure is given by Felippa (2010)

$$\mathbf{K}_M^a = \frac{EA_0}{L_0}\begin{bmatrix} c_m^2 & c_m s_m & -c_m\gamma_m L_0/2 & -c_m^2 & -c_m s_m & -c_m\gamma_m L_0/2 \\ c_m s_m & s_m^2 & -\gamma_m L_0 s_m/2 & -c_m s_m & -s_m^2 & -\gamma_m L_0 s_m/2 \\ -c_m\gamma_m L_0/2 & -\gamma_m L_0 s_m/2 & \gamma_m^2 L_0^2/4 & c_m\gamma_m L_0/2 & \gamma_m L_0 s_m/2 & \gamma_m^2 L_0^2/4 \\ -c_m^2 & -c_m s_m & c_m\gamma_m L_0/2 & c_m^2 & c_m s_m & c_m\gamma_m L_0/2 \\ -c_m s_m & -s_m^2 & \gamma_m L_0 s_m/2 & c_m s_m & s_m^2 & \gamma_m L_0 s_m/2 \\ -c_m\gamma_m L_0/2 & -\gamma_m L_0 s_m/2 & \gamma_m^2 L_0^2/4 & c_m\gamma_m L_0/2 & \gamma_m L_0 s_m/2 & \gamma_m^2 L_0^2/4 \end{bmatrix} \tag{18}$$

$$\mathbf{K}_M^b = \frac{EI_0}{L_0}\begin{bmatrix} 0 & 0 & 0 & 0 & 0 & 0 \\ 0 & 0 & 0 & 0 & 0 & 0 \\ 0 & 0 & 1 & 0 & 0 & -1 \\ 0 & 0 & 0 & 0 & 0 & 0 \\ 0 & 0 & 0 & 0 & 0 & 0 \\ 0 & 0 & -1 & 0 & 0 & 1 \end{bmatrix} \tag{19}$$

$$\mathbf{K}_M^s = \frac{GA_0}{L_0}\begin{bmatrix} s_m^2 & -c_m s_m & -\alpha_1 L_0 s_m/2 & -s_m^2 & c_m s_m & -\alpha_1 L_0 s_m/2 \\ -c_m s_m & c_m^2 & c_m \alpha_1 L_0/2 & c_m s_m & -c_m^2 & c_m \alpha_1 L_0/2 \\ -\alpha_1 L_0 s_m/2 & c_m \alpha_1 L_0/2 & \alpha_1^2 L_0^2/4 & \alpha_1 L_0 s_m/2 & -c_m \alpha_1 L_0/2 & \alpha_1^2 L_0^2/4 \\ -s_m^2 & c_m s_m & \alpha_1 L_0 s_m/2 & s_m^2 & -c_m s_m & \alpha_1 L_0 s_m/2 \\ c_m s_m & -c_m^2 & -c_m \alpha_1 L_0/2 & -c_m s_m & c_m^2 & -c_m \alpha_1 L_0/2 \\ -\alpha_1 L_0 s_m/2 & c_m \alpha_1 L_0/2 & \alpha_1^2 L_0^2/4 & \alpha_1 L_0 s_m/2 & -c_m \alpha_1 L_0/2 & \alpha_1^2 L_0^2/4 \end{bmatrix} \tag{20}$$

where $\alpha_1 = 1 + e_m$. The geometric stiffness matrix K_G remains the same as follows as obtained by Felippa (2010)

$$\mathbf{K}_G = \frac{N_m}{2}\begin{bmatrix} 0 & 0 & s_m & 0 & 0 & s_m \\ 0 & 0 & -c_m & 0 & 0 & -c_m \\ s_m & -c_m & -\frac{1}{2}L_0(1+e_m) & -s_m & c_m & -\frac{1}{2}L_0(1+e_m) \\ 0 & 0 & -s_m & 0 & 0 & -s_m \\ 0 & 0 & c_m & 0 & 0 & c_m \\ s_m & -c_m & -\frac{1}{2}L_0(1+e_m) & -s_m & c_m & -\frac{1}{2}L_0(1+e_m) \end{bmatrix}$$

$$+ \frac{V_m}{2}\begin{bmatrix} 0 & 0 & c_m & 0 & 0 & c_m \\ 0 & 0 & s_m & 0 & 0 & s_m \\ c_m & s_m & -\frac{1}{2}L_0\gamma_m & -c_m & -s_m & -\frac{1}{2}L_0\gamma_m \\ 0 & 0 & -c_m & 0 & 0 & -c_m \\ 0 & 0 & -s_m & 0 & 0 & -s_m \\ c_m & s_m & -\frac{1}{2}L_0\gamma_m & -c_m & s_m & -\frac{1}{2}L_0\gamma_m \end{bmatrix} \tag{21}$$

in which N_m and V_m are the axial and shear forces which are evaluated at the midpoint. The internal nodal force vector is as follows as obtained by Felippa (2010)

$$\mathbf{p} = L_0 \mathbf{B}_m^T \mathbf{z} = \begin{bmatrix} -c_m & -s_m & \frac{1}{2}L_0\gamma_m & c_m & s_m & \frac{1}{2}L_0\gamma_m \\ s_m & -c_m & -\frac{1}{2}L_0(1+e_m) & s_m & -c_m & -\frac{1}{2}L_0(1+e_m) \\ 0 & 0 & -1 & 0 & 0 & 1 \end{bmatrix}^T \begin{bmatrix} N \\ V \\ M \end{bmatrix} \tag{22}$$

where $\mathbf{z}^T = [N \;\; V \;\; M]$. The external nodal force vector can be expressed as follows

$$\mathbf{f} = h_e \int_h \int_{L_0} \begin{bmatrix} 1-\xi_1 & 0 & 0 \\ 0 & 1-\xi_1 & 0 \\ 0 & 0 & 1-\xi_1 \\ 1-\xi_2 & 0 & 0 \\ 0 & 1-\xi_2 & 0 \\ 0 & 0 & 1-\xi_2 \end{bmatrix} \begin{bmatrix} f_X \\ f_Y \\ 0 \end{bmatrix} dXdY + h_e \int_{L_0} \begin{bmatrix} 1-\xi_1 & 0 & 0 \\ 0 & 1-\xi_1 & 0 \\ 0 & 0 & 1-\xi_1 \\ 1-\xi_2 & 0 & 0 \\ 0 & 1-\xi_2 & 0 \\ 0 & 0 & 1-\xi_2 \end{bmatrix} \begin{bmatrix} t_X \\ t_Y \\ m_Z \end{bmatrix} dX \tag{23}$$

where f_X,f_Y are the body forces, t_X,t_Y, m_Z are the surface loads in the X, Y directions and about the Z axis, h_e is the thickness, h is the height. In the study, body forces, the surface loads t_X in the X direction and m_Z about the Z axis are taken as zero. For the solution of the total Lagrangian formulations of TL Timoshenko beam element, small-step incremental approaches from known solutions with Newton-Raphson iteration method are used in which the solution for n+1th load increment and ith iteration is obtained in the following form

$$d\mathbf{u}_n^i = (\mathbf{K}_T^i)_S^{-1} (\mathbf{R}_{n+1}^i)_S \tag{24}$$

where $(\mathbf{K}_T^i)_S$ is the system stiffness matrix corresponding to a tangent direction at the ith iteration, $d\mathbf{u}_n^i$ is the solution increment vector at the ith iteration and n+1th load increment, $(\mathbf{R}_{n+1}^i)_S$ is the system residual vector at the ith iteration and n+1th load increment. This iteration procedure is continued until the difference between two successive solution vectors is less than a selected tolerance criterion in Euclidean norm given by

$$\sqrt{\frac{[(d\mathbf{u}_n^{i+1} - d\mathbf{u}_n^i)^T (d\mathbf{u}_n^{i+1} - d\mathbf{u}_n^i)]^2}{[(d\mathbf{u}_n^{i+1})^T (d\mathbf{u}_n^{i+1})]^2}} \le \zeta_{tol} \tag{25}$$

A series of successive approximations gives

$$\mathbf{u}_{n+1}^{i+1} = \mathbf{u}_{n+1}^i + d\mathbf{u}_{n+1}^i = \mathbf{u}_n + \Delta\mathbf{u}_n^i \tag{26}$$

where

$$\Delta\mathbf{u}_n^i = \sum_{k=1}^{i} d\mathbf{u}_n^k \tag{27}$$

The tangent stiffness matrix $(\mathbf{K}_T^i)_e$ for a finite element which are to be used in Eq. (24) at the ith iteration for the total Lagrangian finite element model of TL Timoshenko plane beam element is separated into two parts as follows

$$\mathbf{K}_T = \mathbf{K}_M + \mathbf{K}_G \tag{28}$$

where $\mathbf{K}_M$ is the material stiffness matrix given in explicit form by Eqs. (18)-(20), $\mathbf{K}_G$ is the geometric stiffness matrix given in explicit form by Eq. (21) for the total Lagrangian plane beam element. The residual vector $\mathbf{R}_{n+1}^i$ for a finite element is as follows

$$\mathbf{R}_{n+1}^{i} = \mathbf{f} - \mathbf{p} \tag{29}$$

where **f** is the vector of external forces given by Eq. (23) and **p** is the vector of internal forces given by Eq. (22).

After obtaining the displacements of nodes, the second Piola-Kirchhoff stress tensor components S_{xx}, S_{xy}, S_{yy} can be obtained by using Eq. (7). It is known that the relation between the Cauchy stress tensor components $\sigma_{xx}, \sigma_{xy}, \sigma_{yy}$ and the second Piola-Kirchhoff stress tensor components S_{xx}, S_{xy}, S_{yy} can be written as follows

$$\sigma_{xx} = \frac{^2\rho}{^0\rho}\left(\frac{\partial x}{\partial X}\frac{\partial x}{\partial X}S_{xx} + 2\frac{\partial x}{\partial X}\frac{\partial x}{\partial Y}S_{xy} + \frac{\partial x}{\partial Y}\frac{\partial x}{\partial Y}S_{yy}\right) \tag{30a}$$

$$\sigma_{yy} = \frac{^2\rho}{^0\rho}\left(\frac{\partial y}{\partial X}\frac{\partial y}{\partial X}S_{xx} + 2\frac{\partial y}{\partial X}\frac{\partial y}{\partial Y}S_{xy} + \frac{\partial y}{\partial Y}\frac{\partial y}{\partial Y}S_{yy}\right) \tag{30b}$$

$$\sigma_{xy} = \frac{^2\rho}{^0\rho}\left(\frac{\partial x}{\partial X}\frac{\partial x}{\partial X}S_{xx} + 2\frac{\partial X}{\partial X}\frac{\partial y}{\partial Y}S_{xy} + \frac{\partial x}{\partial Y}\frac{\partial y}{\partial Y}S_{yy}\right) \tag{30c}$$

where $^0\rho$ and ρ represent the mass densities of the material in configurations C_0 and C, respectively. The relations between the Lagrange coordinates X, Y and Euler coordinates x, y are given by Eqs. (1), (2). The relation between $^0\rho$ and ρ is as follows

$$^0\rho = \rho J \tag{31}$$

where J is the determinant of the deformation gradient tensor **F** (or the Jacobian of the transformation) and defined as follows

$$J = \det(\mathbf{F}) = \begin{vmatrix} \frac{\partial x}{\partial X} & \frac{\partial x}{\partial Y} & \frac{\partial x}{\partial Z} \\ \frac{\partial y}{\partial X} & \frac{\partial y}{\partial Y} & \frac{\partial y}{\partial Z} \\ \frac{\partial z}{\partial X} & \frac{\partial z}{\partial Y} & \frac{\partial z}{\partial Z} \end{vmatrix} \tag{32}$$

In this study, it is assumed that $^0\rho = \rho$.

The beams considered in numerical examples are elastic, with undeformed length L, rectangular cross-section of width b and thickness h (see Fig. 1).

The dimensionless quantities can be expressed as

$$\xi = \frac{X}{L}, \quad \eta = \frac{Y}{L}, \quad U = \frac{u_x}{L}, \quad V = \frac{u_y}{L}$$

$$\tau_M = 12\delta^2\alpha_x T_M, \quad \tau_D = 12\delta^2\alpha_x T_D$$

$$P_H = \frac{p_H L^2}{EI}, \quad P_V = \frac{p_V L^2}{EI}, \quad M = \frac{mL}{EI}$$

$$\bar{\sigma}_{XX} = \frac{\sigma_{XX}}{ET_M\alpha_x}, \quad \bar{\sigma}_{XY} = \frac{\sigma_{XY}}{ET_M\alpha_x} \tag{33}$$

Where P_H is dimensionless constraint force in the horizontal direction, P_V is dimensionless constraint force in the vertical direction, M is dimensionless constraint moment, $\overline{\sigma}_{XX}$ is dimensionless Cauchy normal stress, $\overline{\sigma}_{XY}$ is dimensionless shear stress and δ is the ratio of L/h (lenght/height).

When $\tau_D = 0$, then the temperature rise is uniform.

3. Numerical results

In the numerical examples, the geometrically non-linear static deflections as well as the Cauchy normal and the Cauchy shear stresses are calculated and presented in figures. To this end, by use of usual assembly process, the system tangent stiffness matrix and the system residual vector are obtained by using the element stiffness matrixes and element residual vectors for the total Lagrangian Timoshenko plane beam element. After that, the solution process outlined in the previous section is used for obtaining the related solutions for the total Lagrangian finite element model of Timoshenko plane beam element. The beams considered in numerical examples are made of lower-carbon steel: Coefficient of thermal expansion is taken as $\alpha_X = 12 \times 12^{-6}\ 1/^{o}\mathrm{C}$, Young's modulus is taken as E = 210 GPa, Poisson's ratio is taken as ν = 0.2875. Convergence and comparison studies are also performed. In the geometrically non-linear case, the Cauchy stresses (true stresses) can be obtained by using Eqs. (30a-c) after obtaining the second Piola-Kirchhoff stresses by using Eq. (7).

In Table 2, the dimensionless central deflections $f = V(0.5)$ of the beam with various boundary conditions under dimensionless non-uniform temperature loading are calculated for various numbers of finite elements for various boundary conditions and number of finite element m for L/h = 5. It is seen from Table 2 that, when the number of finite elements is m = 60, the considered displacements converge perfectly. Therefore, in the numerical calculations, the number of finite elements is taken as m = 60.

Table 2 Convergence analysis for the dimensionless central deflections $f = V(0.5)$ of the beam with various boundary conditions and number of finite elements m for L/h = 5

The dimensionless central deflections $f = V(0.5)$ of the beam						
m	P-P $\tau_M = 70$ $\tau_D = 40$	C-C $\tau_M = 80$ $\tau_D = 60$	P-C $\tau_M = 50$ $\tau_D = 40$	P-G2 $\tau_M = 40$ $\tau_D = 30$	C-G1 $\tau_M = 40$ $\tau_D = 30$	C-G2 $\tau_M = 40$ $\tau_D = 30$
6	0.3108	0.3243	0.2227	0.3121	0.1282	0.2195
10	0.3085	0.3177	0.2207	0.3114	0.1278	0.2184
20	0.3075	0.3149	0.2199	0.3112	0.1277	0.2180
30	0.3073	0.3144	0.2197	0.3111	0.1277	0.2179
40	0.3073	0.3142	0.2197	0.3111	0.1277	0.2178
50	0.3072	0.3142	0.2196	0.3111	0.1277	0.2178
60	0.3072	0.3141	0.2196	0.3111	0.1277	0.2178
70	0.3072	0.3141	0.2196	0.3111	0.1277	0.2178
80	0.3072	0.3141	0.2196	0.3111	0.1277	0.2178

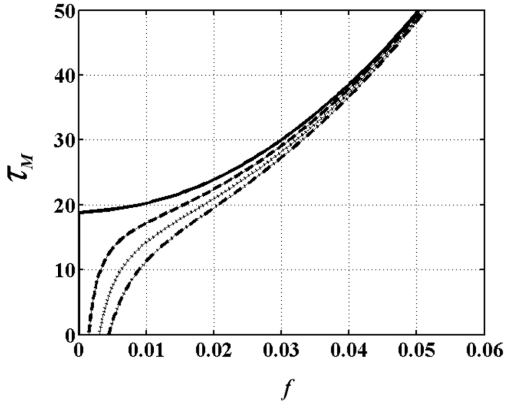

Fig. 5 Dimensionless deflection $f = V(0.4)$ versus mean temperature rise τ_M for given some non-uniform temperature parameter τ_D at $L/h = 20$ and $E/G = 5$ (pinned-fixed).
(——) $\tau_D = 0$, (– – –) $\tau_D = 10$, (·····) $\tau_D = 20$, (–·–·–) $\tau_D = 30$

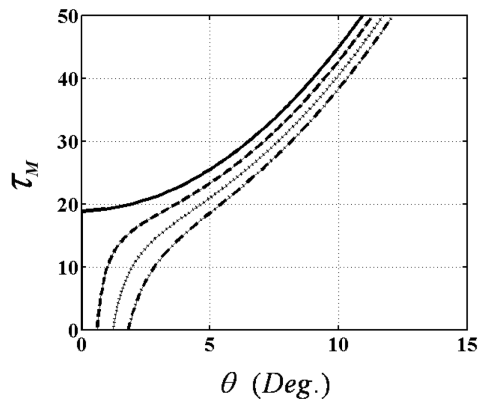

Fig. 6 Left-end rotational angle $\theta = \theta(0)$ (degree) versus mean temperature rise τ_M for given some non-uniform temperature parameter τ_D at $L/h = 20$ and $E/G = 5$ (pinned-fixed).
(——) $\tau_D = 0$, (– – –) $\tau_D = 10$, (·····) $\tau_D = 20$, (–·–·–) $\tau_D = 30$

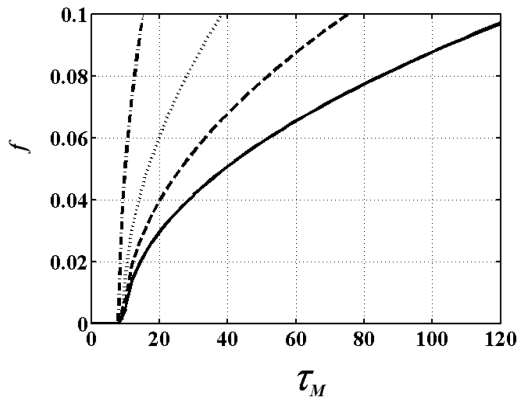

Fig. 7 Dimensionless deflection $f = V(0.5)$ versus mean temperature rise τ_M for some given ratios of L/h for pinned-pinned beam.
(——) $L/h = 20$, (– – –) $L/h = 15$, (·····) $L/h = 10$, (–·–·–) $L/h = 5$

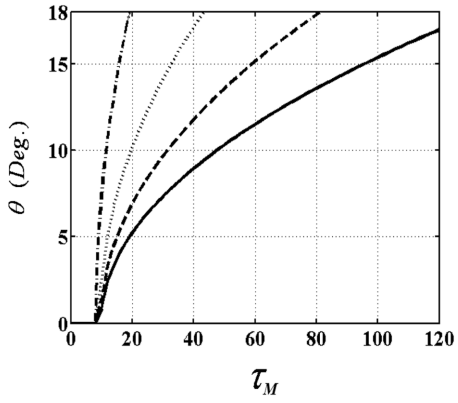

Fig. 8 Left-end rotational angle $\theta = \theta(0)$ (degree) versus mean temperature rise τ_M for some given ratios of L/h for pinned-pinned beam.
(——) $L/h = 20$, (– – –) $L/h = 15$, (·····) $L/h = 10$, (–·–·–) $L/h = 5$

In order to establish the accuracy of the present formulation and the computer program developed by the authors, the results obtained from the present study are compared with the available results in the literature. For this purpose, the dimensionless specified deflections $f = V(0.4)$ and left-end rotational angle $\theta = \theta(0)$ (degree) with various dimensionless non-uniform temperature parameter τ_D for $L/h = 20$ and $E/G = 5$ at pinned-fixed (P-C) beam are calculated and compared with those of Li and Zhou (2003). It is clearly seen that Fig. 5 and Fig. 6 of the present study are the same as Fig. 6(b) and Fig. 7(b) of Li and Zhou (2003).

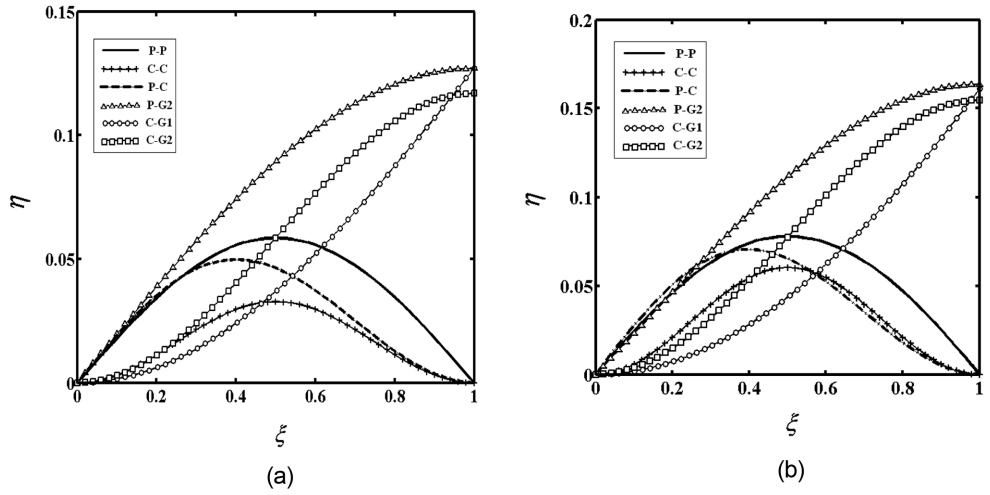

Fig. 9 Thermal buckling configuration of the beam with various boundary conditions for L/h = 20 for (a) τ_M = 50, τ_D = 0, (b) τ_M = 80, τ_D = 30

To further verify the present results, the dimensionless central deflections $f = V(0.5)$ and left-end rotational angle $\theta = \theta(0)$ (degree) versus mean temperature rise τ_M for some given ratio of L/h at pinned-pinned beam are calculated and compared with those of Li and Song (2006) by using the material properties used in Li and Song (2006) under uniform temperature rising. In the study of Li and Song (2006), the ratio of the elasticity modulus and shear modulus is taken as E/G = 206/80. Comparisons of Fig. 7, Fig. 8 with Fig. 1(a), Fig. 2 of Li and Song (2006) show that there is a perfect harmony between the present results and those of Li and Song (2006).

In Fig. 9, the thermal buckled configurations of the beam with various boundary conditions are shown for L/h = 20, τ_M = 50, τ_D = 0, and τ_M = 80, τ_D = 30.

In Table 3, dimensionless central deflections $f = W(0.5)$ and the left-end rotational angle $\phi = \varphi(0)$ (degree) are calculated, respectively, for various dimensionless non-uniform temperature rise τ_D and geometric parameter L/h with various boundary conditions. It is seen from Table 3 that, with increase in the ratio L/h, central dimensionless deflections and rotational angles decrease gradually.

In Table 4, dimensionless end constraint force P_H in the horizontal direction, P_V in the vertical direction and end constraint moment M is calculated, respectively, for various dimensionless non-uniform temperature rise τ_D and geometric parameter L/h for various boundary conditions. It is known that the thermal buckling occurs when the temperature is greater than the critical temperature value, namely when $\tau > \tau_{cr}$. The dimensionless critical buckling temperatures for mean temperature rise τ_M with various boundary conditions for L/h = 20 are obtained and given in Table 5. The values of temperatures given in Table 4 are higher than critical buckling temperatures ($\tau > \tau_{cr}$).

From the mechanical viewpoint, it is evident that P_V = 0 for P-P, C-C, C-G1, C-G2 and P-G2 support conditions. This situation can also be seen from Table 4. It can also be seen from Table 4 that increase in the dimensionless non uniform temperature rise τ_D, causes gradual decrease in the magnitude of dimensionless end constraint forces P_H for all support conditions and P_V for P-C support condition.

Investigation of Table 4 and Figs. 11(a) and 15(a) reveals an interesting result: It is seen from Table 4 that horizontal end constraint force P_H is the same for all the values of τ_D for C-C and C-

Table 3 Variation of the dimensionless central deflections $f = W(0.5)$ and the left-end rotational angle $\phi = \varphi(0)$ (degree) for $\tau_D = 50$ with dimensionless non-uniform temperature rise τ_D and geometric parameter L/h for various boundary conditions

$\tau_M = 50$		L/h					
τ_D	Boundary conditions	10		15		20	
		$f = W(0.5)$	$\theta = \theta(0)$	$f = W(0.5)$	$\theta = \theta(0)$	$f = W(0.5)$	$\theta = \theta(0)$
10	P-P	0.1196	20.5378	0.0789	14.0849	0.0590	10.6796
	C-C	0.0800	0	0.0471	0	0.0332	0
	P-C	0.0976	22.3298	0.0630	15.2101	0.0466	11.5110
	P-G2	0.1816	23.2539	0.1208	15.7202	0.0905	11.8503
	C-G1	0.0781	0	0.0515	0	0.0384	0
	C-G2	0.1188	0	0.0783	0	0.0585	0
15	P-P	0.1199	20.9193	0.0792	14.3290	0.0592	10.8594
	C-C	0.0800	0	0.0471	0	0.0332	0
	P-C	0.0977	22.7393	0.0631	15.4754	0.0467	11.7077
	P-G2	0.1824	23.7923	0.1213	16.0699	0.0909	12.1099
	C-G1	0.0793	0	0.0522	0	0.0390	0
	C-G2	0.1188	0	0.0783	0	0.0585	0
20	P-P	0.1203	21.2976	0.0794	14.5707	0.0594	11.0373
	C-C	0.0800	0	0.0471	0	0.0332	0
	P-C	0.0978	23.1452	0.0632	15.7379	0.0468	11.9023
	P-G2	0.1831	24.3228	0.1218	16.4141	0.0913	12.3654
	C-G1	0.0805	0	0.0530	0	0.0396	0
	C-G2	0.1188	0	0.0783	0	0.0585	0
30	P-P	0.1210	22.0452	0.0799	15.0472	0.0598	11.3878
	C-C	0.0800	0	0.0471	0	0.0332	0
	P-C	0.0980	23.9465	0.0634	16.2551	0.0469	12.2854
	P-G2	0.1844	25.3617	0.1227	17.0876	0.0920	12.8650
	C-G1	0.0831	0	0.0546	0	0.0408	0
	C-G2	0.1188	0	0.0783	0	0.0585	0
50	P-P	0.1222	23.5075	0.0809	15.9750	0.0605	12.0691
	C-C	0.0800	0	0.0471	0	0.0332	0
	P-C	0.0984	25.5119	0.0637	17.2610	0.0472	13.0293
	P-G2	0.1868	27.3598	0.1244	18.3796	0.0932	13.8227
	C-G1	0.0884	0	0.0581	0	0.0434	0
	C-G2	0.1188	0	0.0783	0	0.0585	0

Table 4 Variation of the dimensionless end constraint force PH in the horizontal direction, P_V in the vertical direction and end constraint moment M with dimensionless non-uniform temperature rise τ_D and geometric parameter L/h for $\tau_D = 50$ for various boundary conditions

$\tau_M = 50$		L/h								
	Boundary conditions	10			15			20		
		P_H	P_V	M	P_H	P_V	M	P_H	P_V	M
10	P-P	8.3103	0	0	8.6563	0	0	8.7912	0	0
	C-C	32.1678	0	13.6988	35.5897	0	13.4035	37.1609	0	13.1528
	P-C	16.9707	1.3913	0	18.2592	0.9658	0	18.7977	0.7362	0
	P-G2	1.9748	0	0	2.0159	0	0	2.0310	0	0
	C-G1	2.7927	0	0.7159	2.8445	0	0.4834	2.8635	0	0.3643
	C-G2	9.1458	0	1.0036	9.5238	0	0.8017	9.6717	0	0.6077
15	P-P	7.8969	0	0	8.2273	0	0	8.3560	0	0
	C-C	32.1678	0	14.1154	35.5897	0	13.8202	37.1609	0	13.5694
	P-C	16.6852	1.4340	0	17.9569	0.9946	0	18.4877	0.7579	0
	P-G2	1.7721	0	0	1.8107	0	0	1.8249	0	0
	C-G1	2.9995	0	0.7696	3.0541	0	0.5194	3.0742	0	0.3913
	C-G2	9.1458	0	0.9619	9.5238	0	0.8295	9.6717	0	0.6285
20	P-P	7.4871	0	0	7.8023	0	0	7.9250	0	0
	C-C	32.1678	0	14.5321	35.5897	0	14.2369	37.1609	0	13.9861
	P-C	16.4018	1.4768	0	17.6572	1.0234	0	18.1806	0.7796	0
	P-G2	1.5700	0	0	1.6061	0	0	1.6194	0	0
	C-G1	3.2075	0	0.8236	3.2649	0	0.5556	3.2861	0	0.4185
	C-G2	9.1458	0	0.9203	9.5238	0	0.8572	9.6717	0	0.6493
30	P-P	6.6780	0	0	6.9640	0	0	7.0750	0	0
	C-C	32.1678	0	15.3654	35.5897	0	15.0702	37.1609	0	14.8194
	P-C	15.8408	1.5624	0	17.0650	1.0812	0	17.5741	0.8231	0
	P-G2	1.1672	0	0	1.1986	0	0	1.2101	0	0
	C-G1	3.6275	0	0.9326	3.6908	0	0.6287	3.7141	0	0.4734
	C-G2	9.1458	0	0.8369	9.5238	0	0.9128	9.6717	0	0.6910
50	P-P	5.0975	0	0	5.3287	0	0	5.4180	0	0
	C-C	32.1678	0	17.0321	35.5897	0	16.7369	37.1609	0	16.4861
	P-C	14.7400	1.7341	0	15.9067	1.1968	0	16.3896	0.9101	0
	P-G2	0.1868	0	0	0.3882	0	0	0.3964	0	0
	C-G1	4.4895	0	1.1552	4.5649	0	0.7777	4.5927	0	0.5854
	C-G2	9.1458	0	0.6703	9.5238	0	1.0239	9.6717	0	0.7743

Table 5 The dimensionless critical buckling temperatures for mean temperature rise τ_M with various boundary conditions for L/h = 20

L/h = 20	
Boundary conditions	$\tau_M = \tau_{cr}$
P-P	9.704
C-C	37.14
P-C	19.45
P-G2	2.45
C-G1	2.45
C-G2	9.701

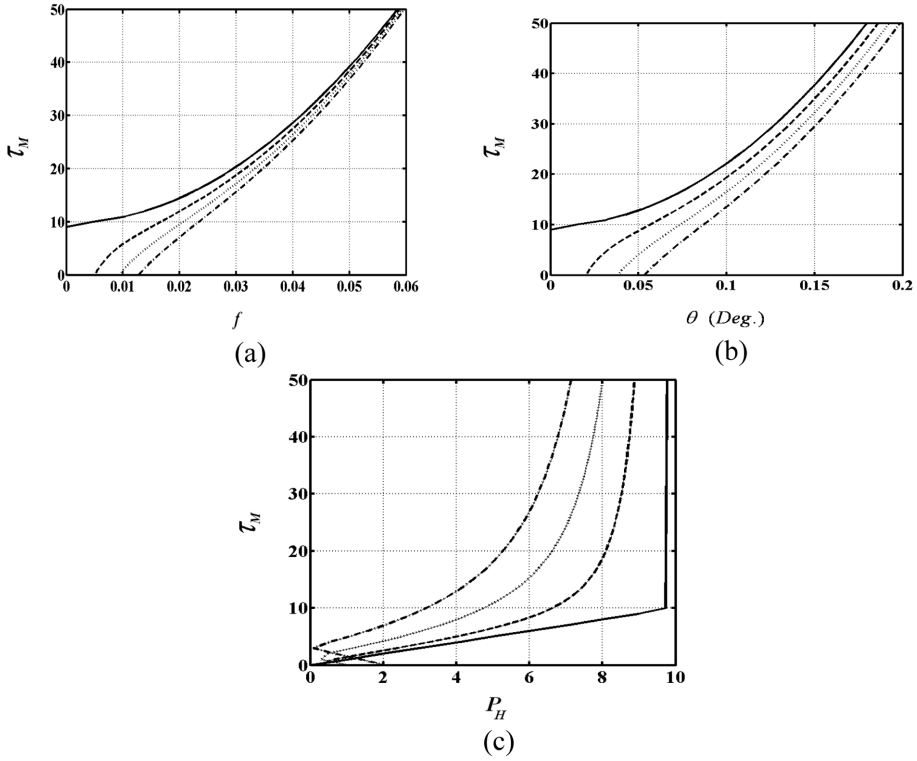

Fig. 10 Dimensionless central deflections $f = W(0.5)$, left-end rotational angle $\phi = \varphi(0)$ (degree) and dimensionless end constraint force P_H in the horizontal direction versus mean temperature rise τ_M for some given non-uniform temperature parameter τ_D for P-P boundary condition at L/h = 20. (a) $f = W(0.5)$ (b) $\phi = \varphi(0)$, (c) P_H
(——) τ_D = 0, (– – –) τ_D = 10, (·····) τ_D = 20, (–·–·–) τ_D = 30

G2 support conditions. It is also seen from Figs. 11(a) and 15(a) that central deflections of the beam are the same for all values of τ_D for C-C and C-G2 support conditions. As far as the authors know, this is a new result. However, it is seen from Table 4 and Figs. 11(b), 15(b) that, the end constraint moment is not the same for C-C and C-G2 support conditions.

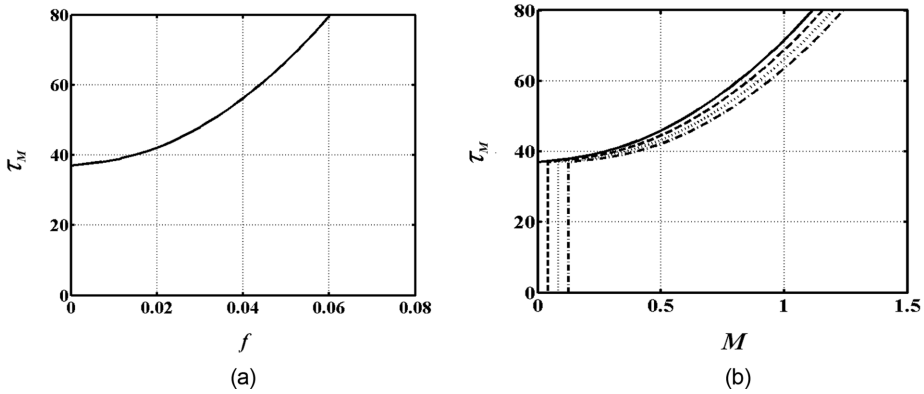

Fig. 11 Dimensionless central deflections $f = W(0.5)$ and dimensionless end constraint moment M versus mean temperature rise τ_M for some given non-uniform temperature parameter τ_D for C-C boundary condition for $L/h = 20$. (a) $f = W(0.5)$, (b) M
(——) $\tau_D = 0$, (– – –) $\tau_D = 10$, (·····) $\tau_D = 20$, (–·–·–) $\tau_D = 30$

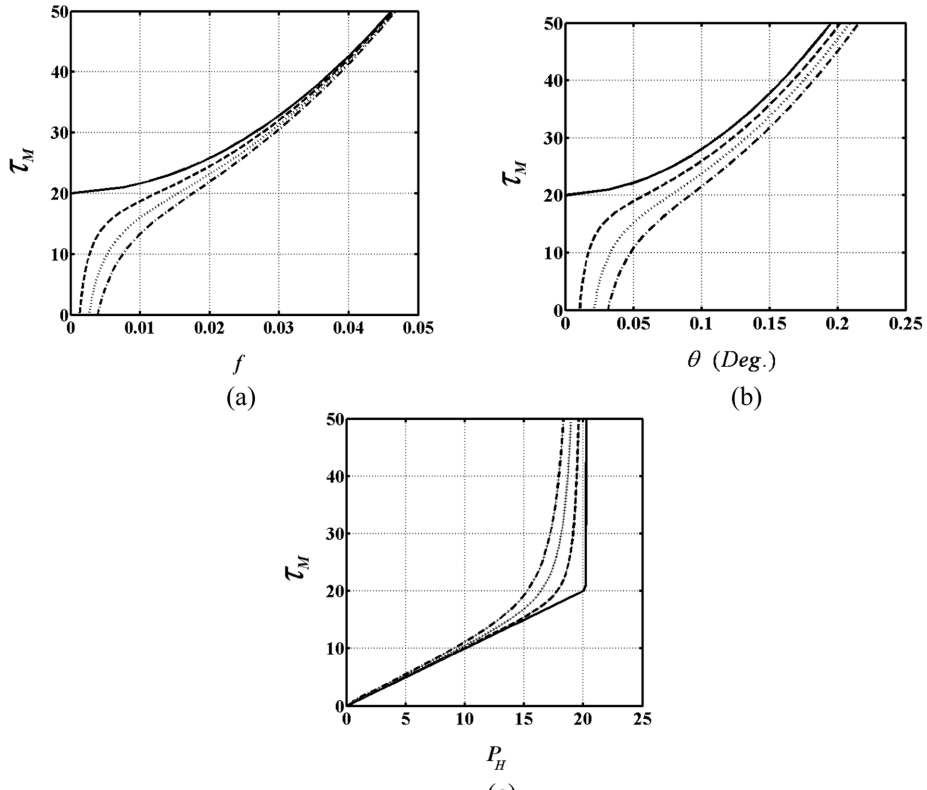

Fig. 12 Dimensionless central deflections $f = W(0.5)$, the left-end rotational angle $\phi = \varphi(0)$ (degree) and dimensionless end constraint force P_H in the horizontal direction versus mean temperature rise τ_M for some given non-uniform temperature parameter τ_D for P-C boundary condition for $L/h = 20$. (a) $f = W(0.5)$, (b) $\phi = \varphi(0)$, (c) P_H
(——) $\tau_D = 0$, (– – –) $\tau_D = 10$, (·····) $\tau_D = 20$, (–·–·–) $\tau_D = 30$

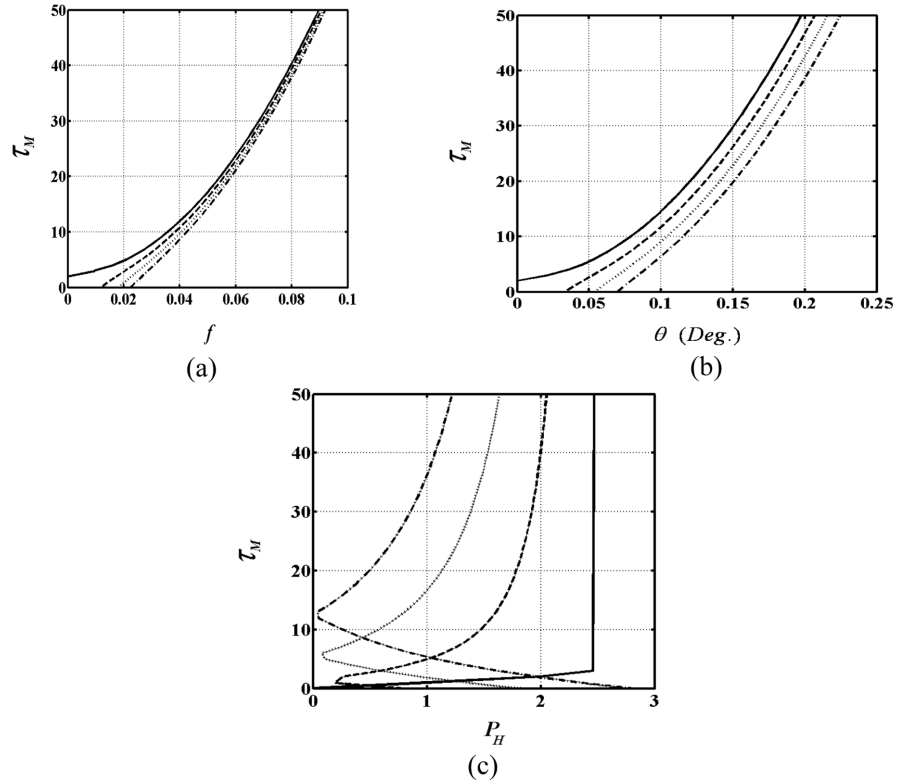

Fig. 13 Dimensionless central deflections $f = W(0.5)$, the left-end rotational angle $\phi = \varphi(0)$ (degree) and dimensionless end constraint force P_H in the horizontal direction versus mean temperature rise τ_M for some given non-uniform temperature parameter τ_D for P-G2 boundary condition for $L/h = 20$. (a) $f = W(0.5)$, (b) $\phi = \varphi(0)$, (c) P_H
(——) $\tau_D = 0$, (– – –) $\tau_D = 10$, (·····) $\tau_D = 20$, (–·–·–) $\tau_D = 30$

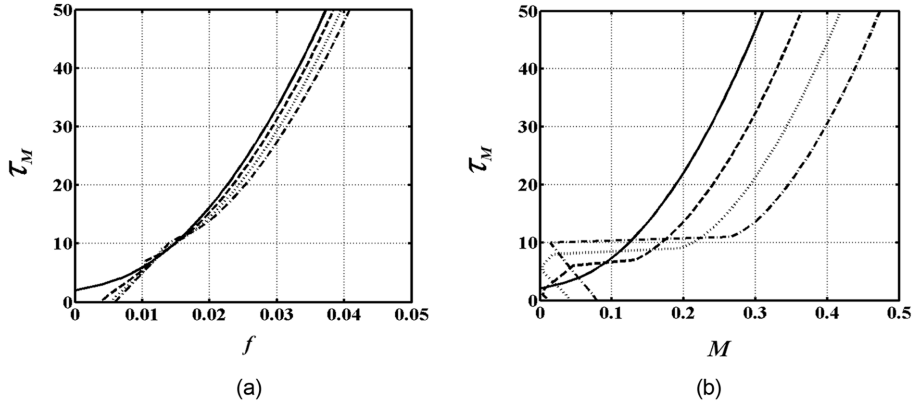

Fig. 14 Dimensionless central deflections $f = W(0.5)$ and dimensionless end constraint moment M versus mean temperature rise τ_M for some given non-uniform temperature parameter τ_D for C-G1 boundary condition for $L/h = 20$. (a) $f = W(0.5)$, (b) M
(——) $\tau_D = 0$, (– – –) $\tau_D = 10$, (·····) $\tau_D = 20$, (–·–·–) $\tau_D = 30$

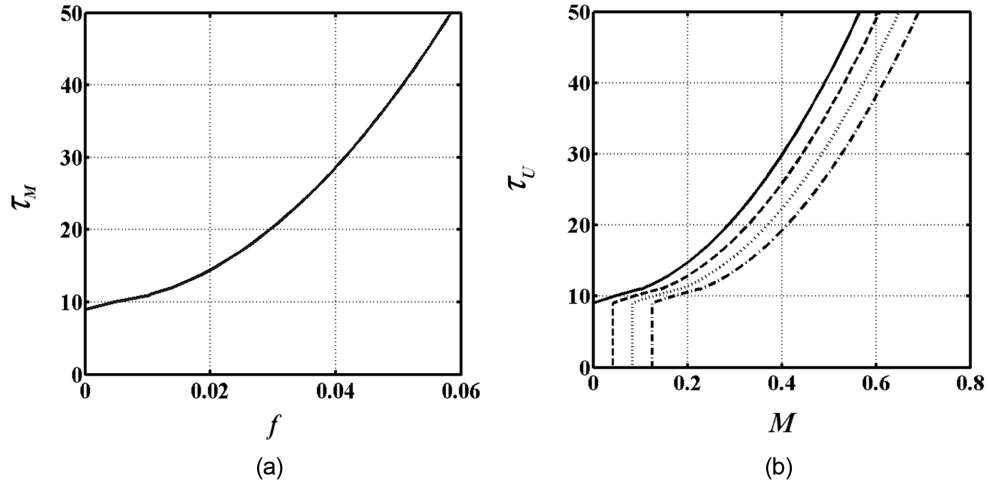

Fig. 15 Dimensionless central deflections $f = W(0.5)$ and dimensionless end constraint moment M versus mean temperature rise τ_M for some given non-uniform temperature parameter τ_D for C-G2 boundary condition for $L/h = 20$. (a) $f = W(0.5)$, (b) M
(——) $\tau_D = 0$, (– – –) $\tau_D = 10$, (·····) $\tau_D = 20$, (–·–·–) $\tau_D = 30$

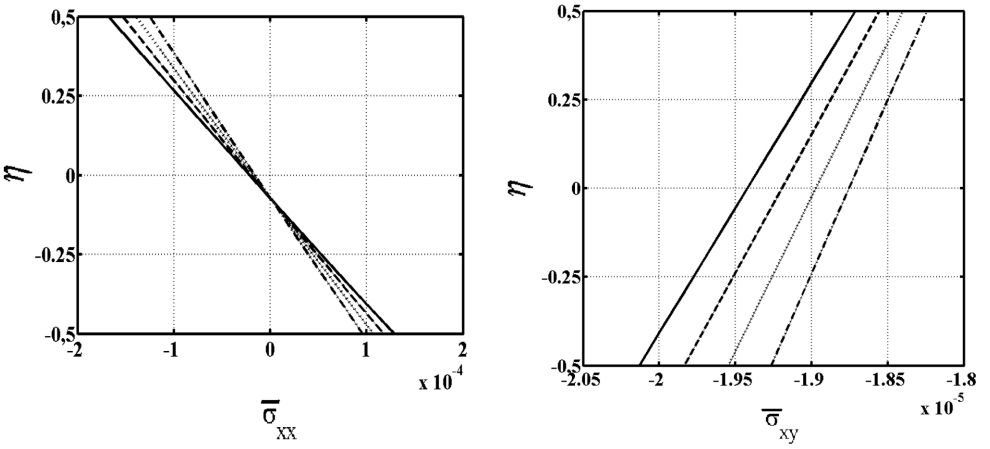

Fig. 16 Stress distributions versus mean temperature rise τ_M for some given non-uniform temperature parameter τ_D at central section, $\xi = 0.5$, for $L/h = 20$ for P-P. (a) Dimensionless Cauchy normal stress (b) Dimensionless Cauchy shear stress
(——) $\tau_D = 0$, (– – –) $\tau_D = 10$, (·····) $\tau_D = 20$, (–·–·–) $\tau_D = 30$

It is seen from Figs. 12, 13 and 14 that central deflections, end constraint forces and end constraint moments varies with variation of τ_D for P-C, P-G2, C-G1 boundary conditions.

The superiority or advantage of the finite element method to the other methods is that in the finite element method, all the boundary conditions can be taken into consideration without any difficulty.

In Figs. 16-21, dimensionless Cauchy normal stresses and dimensionless Cauchy shear stresses are

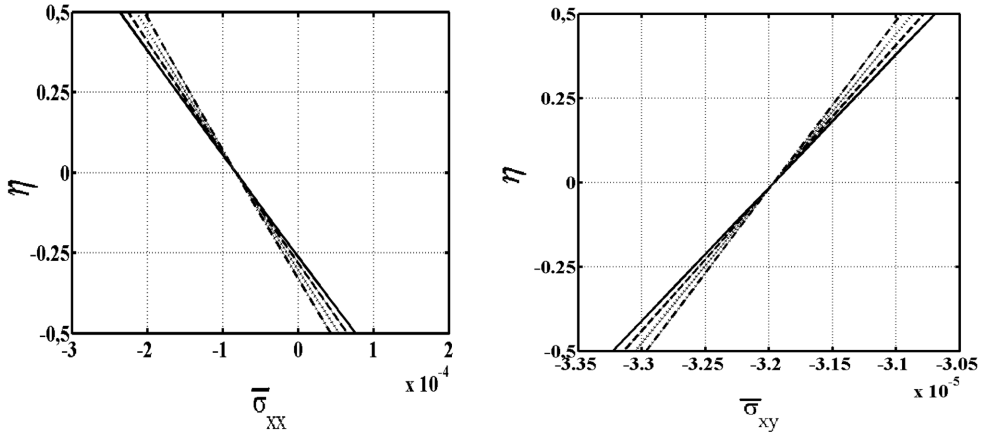

Fig. 17 Stress distributions versus mean temperature rise τ_M for some given non-uniform temperature parameter τ_D at central section, ξ = 0.5, for L/h = 20 for C-C. (a) Dimensionless Cauchy normal stress (b) Dimensionless Cauchy shear stress
(——) τ_D = 0, (– – –) τ_D = 10, (·····) τ_D = 20, (–·–·–) τ_D = 30

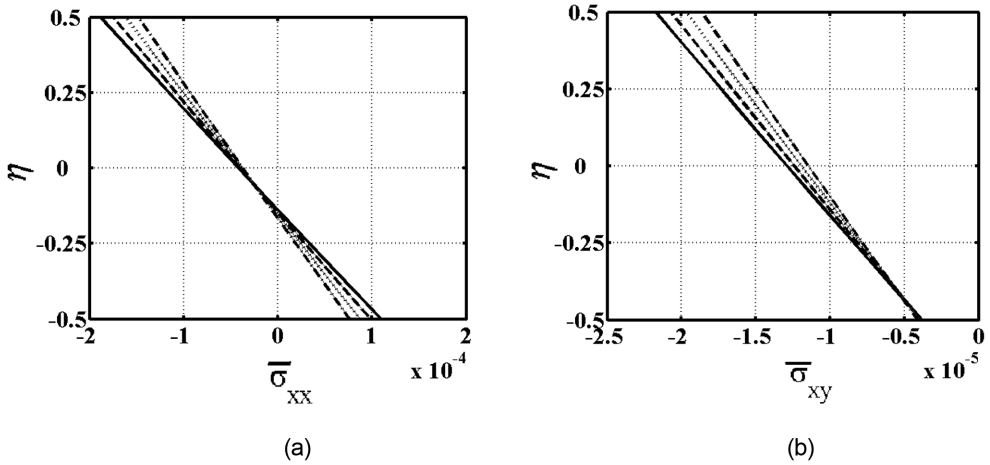

Fig. 18 Stress distributions versus mean temperature rise τ_M for some given non-uniform temperature parameter τ_D at central section, ξ = 0.5, for L/h = 20 for P-C. (a) Dimensionless Cauchy normal stress, (b) Dimensionless Cauchy shear stress
(——) τ_D = 0, (– – –) τ_D = 10, (·····) τ_D = 20, (–·–·–) τ_D = 30

given at the central section, ξ = 0.5, for L/h = 20 for various support conditions. As it is expected, the Cauchy normal stresses are not zero at Y = 0 ($\sigma_{xx} \neq 0$ at $Y = 0$) in the case of temperature rise as seen from Figs. 16(a)-21(a). It is known that the shear stress distribution for the Timoshenko beam in the geometrically linear case is constant along the Y axis. However, the shear stress distribution for the Timoshenko beam is not constant along the Y axis in the geometrically nonlinear case and changes linearly along the Y axis as seen from Figs. 16(b)-21(b).

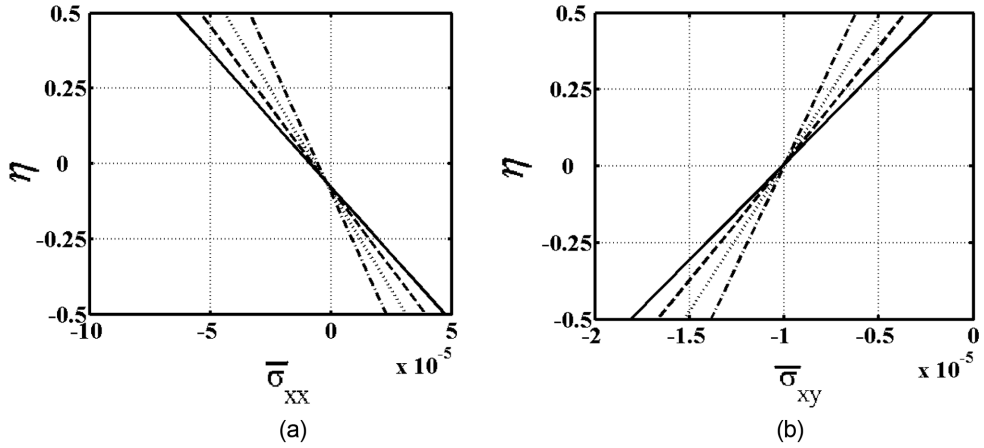

Fig. 19 Stress distributions versus mean temperature rise τ_M for some given non-uniform temperature parameter τ_D at central section, $\xi = 0.5$, for $L/h = 20$ for P-G2. (a) Dimensionless Cauchy normal stress (b) Dimensionless Cauchy shear stress
(——) $\tau_D = 0$, (– – –) $\tau_D = 10$, (·····) $\tau_D = 20$, (–·–·–) $\tau_D = 30$

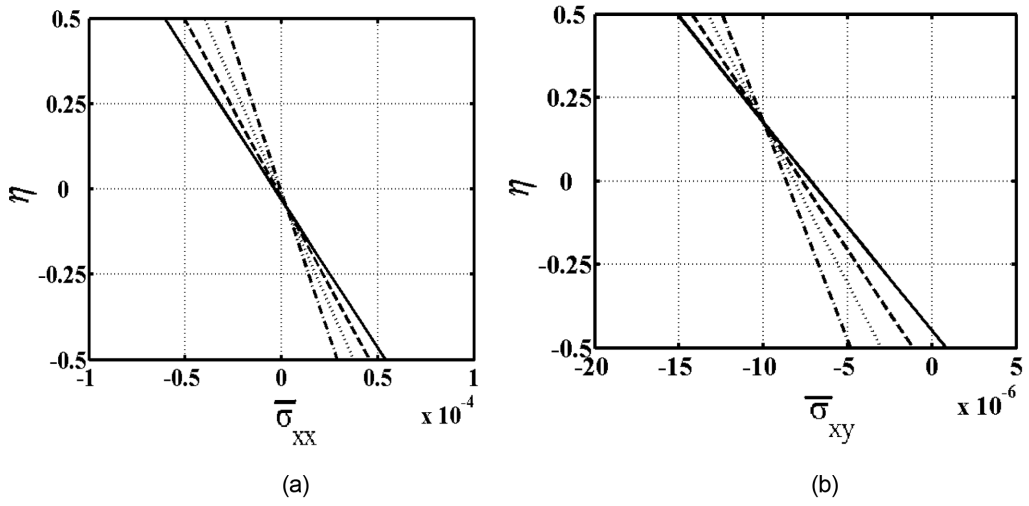

Fig. 20 Stress distributions versus mean temperature rise τ_M for some given non-uniform temperature parameter τ_D at central section, $\xi = 0.5$, for $L/h = 20$ for C-G1. (a) Dimensionless Cauchy normal stress, (b) Dimensionless Cauchy shear stress
(——) $\tau_D = 0$, (– – –) $\tau_D = 10$, (·····) $\tau_D = 20$, (–·–·–) $\tau_D = 30$

When the beam is in a bent configuration with negative displacements and when the temperature rise of the top side of the beam is greater than the temperature rise of the bottom side of the beam, then increase in τ_D causes decrease in the absolute values of Cauchy normal stresses and Cauchy shear stresses. If the beam was in a bent configuration with positive displacements and when the temperature rise of the top side of the beam was greater than the temperature rise of the bottom side of the beam, then increase in τ_D would cause increase in the absolute values of Cauchy normal

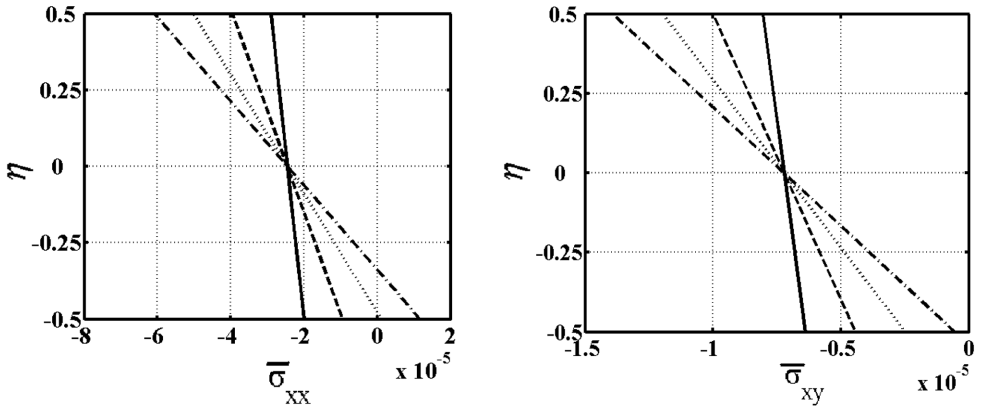

Fig. 21 Stress distributions versus mean temperature rise τ_D for some given non-uniform temperature parameter τ_M at central section, $\xi = 0.5$, for $L/h = 20$ for C-G2. (a) Dimensionless Cauchy normal stress, (b) Dimensionless Cauchy shear stress
(——) $\tau_D = 0$, (– – –) $\tau_D = 10$, (·····) $\tau_D = 20$, (–·–·–) $\tau_D = 30$

stresses and Cauchy shear stresses.

4. Conclusions

This paper focuses on post-buckling analysis of Timoshenko beams with various boundary conditions subjected to a non-uniform thermal loading by using the total Lagrangian Timoshenko beam element approximation. Six type of support conditions for the beams are considered. The considered highly non-linear problem is solved by using incremental displacement-based finite element method in conjunction with Newton-Raphson iteration method. The convergence studies are made and the obtained results are compared with the published results.

As far as the authors know, there is no study on the post-buckling analysis of Timoshenko beams under uniform and non-uniform thermal loading considering full geometric non-linearity investigated by using finite element method: Gupta *et al*. (2009) investigated the post-buckling analysis of beams under thermal loading by using finite element method and von-Karman strain-displacement approximation in which full geometric non-linearity can not be considered. In this study, the post buckling analysis of Timoshenko beams under non-uniform thermal loading with various boundary conditions is considered by using total Lagrangian finite element method in which full geometric nonlinearity can be considered as distinct from the study of Gupta *et al*. (2009). The support reactions, displacements of the midpoint of the beam and the rotations of the left end supports are calculated. It is found that non-uniformity of temperature rise does not affect the horizontal and vertical support reactions in some support conditions. Also, Cauchy normal stresses and Cauchy shear stresses are calculated.

The superiority or advantage of the finite element method to the other methods is that in the finite element method, all the boundary conditions can be taken into consideration without any difficulty.

References

Akbaş Ş.D. and Kocatürk, T. (2011), "Post-buckling analysis of a simply supported beam under uniform thermal loading", *Sci. Res. Essay.,* **6**(4), 1135-1142.

Aristizabal-Ochoa, J.D. (2007), "Large deflection and post-buckling behavior of Timoshenko beam-columns with semi-rigid connections including shear and axial effects", *J. Eng. Struct.,* **29**(6), 991-1003.

Aristizabal-Ochoa, J.D. (2008), "Slope-deflection equations for stability and second- order analysis of Timoshenko beam-column structures with semi-rigid connections", *J. Eng. Struct.,* **30**(9), 2517-2527.

Aristizabal-Ochoa, J.D. (2008), "Closure: slope-deflection equations for stability and second-order analysis of Timoshenko beam-column structures with semi-rigid connections", *J. Eng. Struct.*, **30**(11), 3394-3395.

Chen, B., Gu, Y., Zhao, G., Lin, W., Chang, T.Y.P. and Kuang, J.S. (2003), "Design optimization for structural thermal buckling", *J. Therm. Stresses,* **26**(5), 479-494.

Coffin, D.W. and Bloom, F. (1999), "Elastica solution for the hygrothermal buckling of a beam", *Int. J. Nonlin. Mech.,* **34**(5), 935-947.

Evandro, P. Jr. and Joao, B.M.S. (2008), "Desing sensitivity analysis of nonlinear structures subjected to thermal loads", *Comput. Struct.,* **86**(11-12), 1369-1384.

Felippa, C.A. (2010), "Notes on nonlinear finite element methods", http://www.colorado. edu/engineering/cas/courses.d/NFEM.d/NFEM.Ch09.d/NFEM.Ch09.pdf

Gauss, R.C. and Antman, S.S. (1984), "Large thermal buckling of non-uniform beam and plates", *Int. J. Solids Struct.*, **20**(11-12), 979-1000.

Gupta, R.K., Gunda, J. B., Janardhan, G.R. and Rao, G.V. (2009), "Comparative study of thermal post-buckling analysis of uniform slender & shear flexible columns using rigorous finite element and intutive formulations", *Int. J. Mech. Sci.,* **51**(3), 204-212.

Gupta, R.K., Gunda, J.B., Janardhan, G.R. and Rao, G.V. (2010), "Post-buckling analysis of composite beams: Simple and accurate closed-form expressions", *Compos. Struct.,* **92**(3), 1947-1956.

Gupta, R.K., Gunda, J.B., Janardhan, G.R. and Rao, G.V. (2010), "Thermal Post-buckling analysis of slender columns using the concept of coupled displacement field", *Int. J. Mech. Sci.,* **52**(4), 590-594.

Jekot, T. (1996), "Non-linear problems of thermal buckling of a beam", *J. Therm. Stresses*, **19**, 359-369.

Li, S.R. (2000), "Thermal post-buckling of asymmetrically supported elastic rods", *Eng. Mach.,* **17**(5), 115-119.

Li, S. and Cheng, C. (2000), "Analysis of thermal post-buckling of heated elastic rods", *Appl. Math. Mech. (English ed.)*, **21**(2), 133-140.

Li, S., Zhou, Y.H. and Zheng, X. (2002), "Thermal post- buckling of a heated elastic rod with pinned-fixed ends", *J. Therm. Stresses*, **25**(1), 45-56.

Li, S. and Zhou, Y. (2001), "Thermal post-buckling of rods with variable cross sections", *Proceedings of the Fourth International Congress on Thermal Stresses*, Osaka, Japan.

Li, S.R., Cheng, C.J. and Zhou, Y.H. (2003), "Thermal post-buckling of an elastic beams subjected to a transversely non-uniform temperature rising", *Appl. Math. Mech. (English ed.)*, **24**(5), 514-520.

Li, S. and Zhou, Y. (2003), "Geometrically nonlinear analysis of Timoshenko beams under thermomechanical loadings", *J. Therm. Stresses*, **26**(9), 861-872.

Li, S. and Song, X. (2006), "Large thermal deflections of Timoshenko beams under transversely non-uniform temperature rise", *Mech. Res. Comm.*, **33**(1), 84-92.

Rao, G.V. and Raju, K.K. (1984), "Thermal postbuckling of columns", *AIAA J.*, **22**(6), 850-851.

Reddy, J.N. (2004), *An Introduction to Non-linear Finite Element Analysis*, Oxford University Press Inc., New York.

Song, X. and Li, S.R. (2007), "Thermal buckling and post-buckling of pinned-fixed Euler-Bernoulli beams on an elastic foundation", *Mech. Res. Comm.,* **34**(2), 164-171.

Vaz, M.A. and Solano, R.F. (2003), "Postbuckling analysis of slender elastic rods subjected to uniform thermal loads", *J. Therm. Stresses*, **26**(9), 847-860.

Vaz, M.A. and Solano, R.F. (2004), "Thermal post-buckling of slender elastic rods with hinged ends constrained by a linear spring", *J. Therm. Stresses,* **27**(4), 367-380.

Vaz, M.A., Nascimento, M.S. and Solano, R.F. (2007), "Initial post-buckling of elastic rods subjected to thermal loads and resting on an elastic foundation", *J. Therm. Stresses,* **30**(4), 381-393.

Vaz, M.A., Cyrino, J.C.R. and Neves, A.C. (2010), "Initial thermo-mechanicalpost-buckling of beams with temperature-dependent physical properties", *Int. J. Nonlin. Mech.,* **45**(3), 256-262.
Zienkiewichz, O.C. and Taylor, R.L. (2000), *The Finite Element Method*, Fifth Edition, Volume 2: Solid Mechanics, Butterworth-Heinemann, Oxford.